Organic & Biomolecular Chemistry

PAPER

View Article Online
View Journal | View Issue

Cite this: *Org. Biomol. Chem.*, 2015, **13**, 6984

Aggregation of asphaltene model compounds using a porphyrin tethered to a carboxylic acid†

Matthias Schulze,[a] Marc P. Lechner,[a] Jeffrey M. Stryker[b] and Rik R. Tykwinski*[a]

Received 25th April 2015,
Accepted 19th May 2015

DOI: 10.1039/c5ob00836k

www.rsc.org/obc

A Ni(II) porphyrin functionalized with an alkyl carboxylic acid (**3**) has been synthesized to model the chemical behavior of the heaviest portion of petroleum, the asphaltenes. Specifically, porphyrin **3** is used in spectroscopic studies to probe aggregation with a second asphaltene model compound containing basic nitrogen (**4**), designed to mimic asphaltene behavior. NMR spectroscopy documents self-association of the porphyrin and aggregation with the second model compound in solution, and a Job's plot suggests a 1 : 2 stoichiometry for compounds **3** and **4**.

Introduction

The foreseeable exhaustion of conventional fossil fuels has resulted in an increasing focus on efficient use of alternative petroleum sources, such as heavy crude oil.[1] In order to convert heavy oil to valuable fuels, however, significant upgrading is required,[2] and these processes are hampered by the heaviest and most problematic component of heavy oil, the asphaltenes.[3] Asphaltenes are commonly known to cause problems for a variety of practical processes, such as transportation, storage, and refining.[2–4] To solve these issues, significant efforts have been expended to understand the bulk behavior of asphaltenes,[2,4,5] and these efforts have even suggested that the carbon-rich and heteroatom doped composition of asphaltenes might yield materials for electronic devices.[6,7] In spite of these studies, however, the general molecular structure of the asphaltenes remains to be resolved,[8] and a major barrier to this goal is the formation of very stable aggregates between individual molecules that complicates many analysis techniques.[9]

For almost a century, it has been suggested and, for the most part, accepted that asphaltenes are composed of large aromatic cores that also contain heteroaromatics and metalloporphyrins, with a molecular weight (MW) of *ca.* 750 g mol^{-1} (Fig. 1a). These large aromatic islands are then surrounded by functional groups, including alkyl groups and alkyl carboxylic acids.[10–12] This paradigm gives rise to the "continental" or "island" model (more specifically the Yen–Mullins model), and it is believed that aggregation in these types of molecules is driven primarily by π–π stacking interactions.[13]

Alternatively, an archipelago model for the asphaltenes has been introduced, in which smaller aromatic islands are tethered together by alkyl chains (Fig. 1b).[8] In the case of archipelago asphaltenes, it has been hypothesized that aggregation results from the cumulative effect of numerous intermolecular stabilizing forces, which might include, among others, π–π-stacking, axial coordination of metalloporphyrins, hydrogen bonding, hydrophobic interactions, and acid–base interactions.[8]

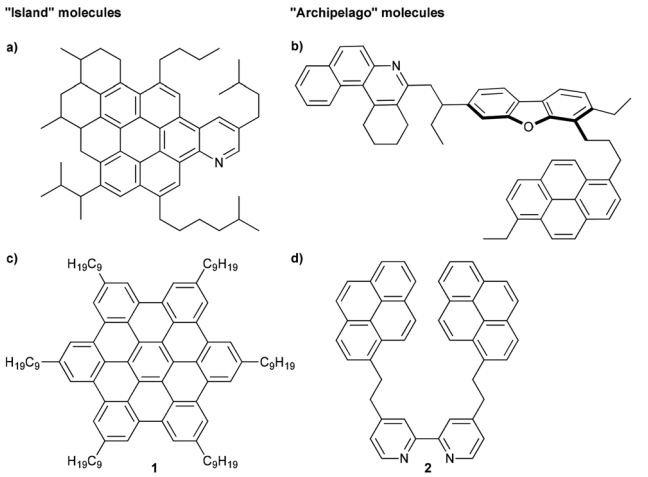

Fig. 1 Schematic example of an (a) island asphaltene compound (MW = 756 g mol^{-1}) from ref. 13 and (b) archipelago asphaltene compound (MW = 754 g mol^{-1}) from ref. 8. Examples of model compounds used to study aggregation of asphaltenes, representing (c) island (MW = 1280 g mol^{-1})[14] and (d) archipelago (MW = 613 g mol^{-1})[15] structures.

[a]*Department of Chemistry and Pharmacy & Interdisciplinary Center of Molecular Materials (ICMM), Friedrich-Alexander-Universität Erlangen-Nürnberg (FAU), Henkestraße 42, 91054 Erlangen, Germany. E-mail: rik.tykwinski@fau.de; Fax: +49-9131-85-26865; Tel: +49-9131-85-22540*

[b]*Department of Chemistry, University of Alberta, Edmonton, Alberta T6G 2G2, Canada*

†Electronic supplementary information (ESI) available: NMR spectra of compounds **3–10**, 2D NMR spectra of compound **4**, as well as experimental details and NMR data of the aggregation studies. See DOI: 10.1039/c5ob00836k

Much of the support for the island model comes from a "top-down" approach, *i.e.*, the study of natural asphaltene samples by various physical and analytical methods.[13] Evidence for the archipelago model using the "top-down" approach has also been reported, including ruthenium-ion-catalyzed oxidation (RICO) experiments,[16–18] small-angle neutron scattering,[19,20] calculations,[21,22] and thermal cracking experiments.[23,24] We hypothesize that a "bottom-up" approach, is paramount to understanding asphaltene aggregation on a molecular level. While the "top-down" approach looks at properties of the bulk material, a "bottom-up" study targets specific molecules with functionalities found in asphaltenes (Fig. 1c and d).[25] With the exact structure of the molecules known, physical properties can be investigated at a molecular level. This tactic is quite common in supramolecular materials chemistry,[26–28] for example, and should be useful toward deciphering specific intermolecular interactions related to the asphaltene aggregation, regardless of whether the continental or the archipelago motif is being considered. There are, however, surprisingly only a few efforts reported in the literature that describe the rational synthesis of compounds specifically to mimic the behavior of asphaltenes.[15,29–31] Rather, existing molecules are often employed, presumably out of convenience, to emulate asphaltene molecules. For example, hexabenzocoronenes (HBCs) substituted with alkyl chains (**1**) have been used in studies by Gray and Müllen to represent molecules of the continental model, and such HBCs show dimer formation in organic solvents (Fig. 1c),[8,14,32] while Anisimov examined the aggregation behavior of a *tert*-butyl substituted HBC.[33] HBCs, however, have an aromatic core built from 13 fused rings, and the majority of asphaltene molecules are expected to have only 4 to 10 fused rings.[34,35] Akbarzadeh *et al.* have used smaller ring systems (alkyl bridged pyrene model compounds) either with or without heteroatoms,[29] and only structures with heteroatoms form dimers in organic solvents. In line with these results, Tan *et al.* have described that the 2,2′-bipyridine derivative **2** forms dimers both in solution and in the solid state (Fig. 1d),[15] and it is suggested that water enhances dimer formation, presumably by the formation of hydrogen bonding, bridging the heteroatoms between two individual molecules.[30] Experimental results were also supported by density functional theory and 3D-RISM-KH calculations.[36,37]

Studies to date with model asphaltene compounds, as briefly summarized in the preceding paragraphs, are not fully consistent with the view that asphaltene aggregation is dominated by π-stacking. Given the acknowledged structural diversity of the asphaltenes, it seems likely that intermolecular associations might be better described by multiple cooperative interactions facilitated by heteroatoms and functional groups.[8] An obvious target under this premise is the interaction of an acid and a base, as expected in natural asphaltenes, for example, between pyridyl and carboxylic acid groups.[12,38] To explore this concept, in the current study two model compounds have been chosen, an acid and a base (Fig. 2). A porphyrin group has been chosen as a platform for the acid moiety, namely compound **3**. Porphyrins are known to exist in petroleum since the pioneering work by Treibs in 1934,[39–42] and these so-called petroporphyrins are mainly observed as V(IV)O and Ni(II) species.[12,43] To the best of our knowledge, however, only simple, unfunctionalized, and commercially available porphyrins have been employed to model asphaltene aggregation.[44] Archipelago-type porphyrins have been used for the investigation of thermal cracking behavior,[45] but there are no studies that report a synthetic strategy specifically designed for porphyrins that enable the study of asphaltene aggregation.[26] It is worth noting the extensive synthetic porphyrins independently reported by Clezy and Lash to serve as model compounds for petroporphyrins, albeit without a focus on aggregation.[46–48]

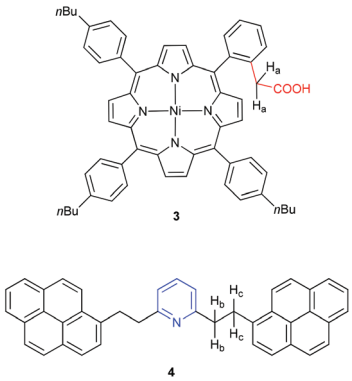

Fig. 2 Model compounds under study to probe aggregation based on the interactions of an acid (**3**) and base (**4**).[49]

To explore the aggregation behavior of porphyrin **3**, it is combined with a compound that features a basic nitrogen group. Namely, we have chosen archipelago model compound **4** (Fig. 2), in which the pyridyl-ring is combined with large aromatic groups appended *via* flexible alkyl tethers. Binding studies by NMR spectroscopy show self-association of porphyrin **3** and the formation of an aggregate between **3** and **4** in solution, demonstrating the potential of this aggregation motif for native asphaltenes.

Results and discussion

Synthesis

Aldehyde **5** (Scheme 1) was synthesized from 1-bromo-2-(methoxymethyl)benzene as described by Ullenius and coworkers.[50] Subsequently, aldehyde **5**, commercial 4-*n*-butylbenzaldehyde (**6**), and pyrrole were used in a mixed porphyrin condensation with $BF_3{\cdot}OEt_2$ as a Lewis-acid and EtOH as a co-catalyst, followed by oxidation with DDQ, according to procedures reported by Lindsey[51] and Jux.[52] From this reaction, the unsymmetrical methoxymethyl substituted porphyrin **7a** and the symmetrical derivative **8**[53] were isolated in significant yields. The desired target, porphyrin **7a**, was then reacted with HBr in AcOH, according to a procedure by Jux,[52] to give

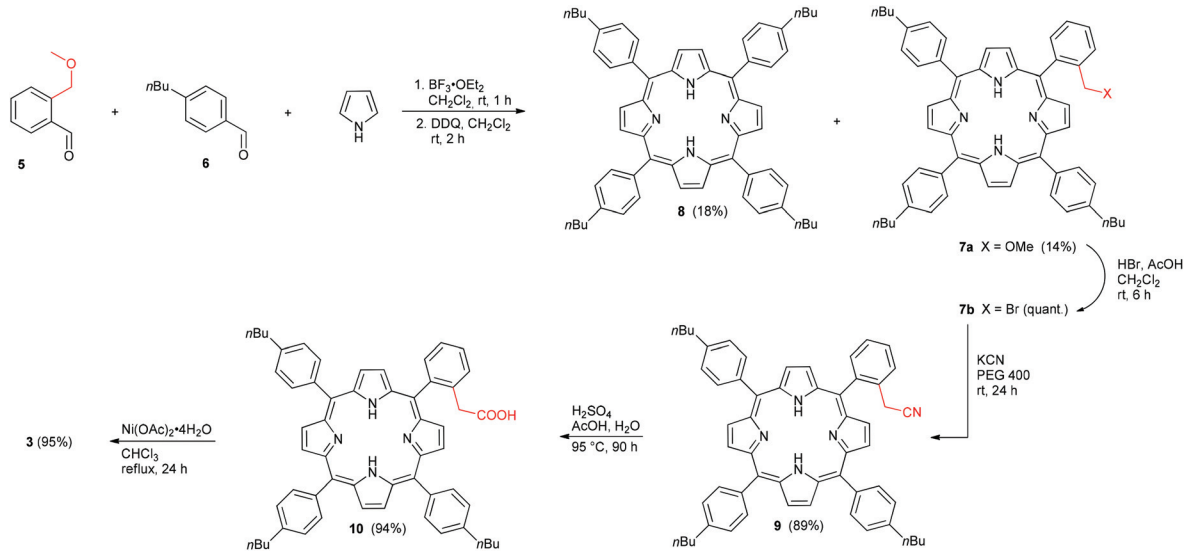

Scheme 1 Synthesis of the Ni(II) porphyrin **3** featuring an alkyl carboxylic acid group.

bromide **7b**, which was used without further purification. The route of Jasinski *et al.* for cyanation of bromomethyl TPPs was modified slightly,[54] and treatment of the crude bromide **7b** with KCN in PEG 400 gave the cyanomethyl substituted porphyrin **9** in excellent yield. Hydrolysis of the nitrile **9** under acidic conditions yielded the carboxylic acid, and the free base porphyrin **10** was isolated in good yield *via* column chromatography. Conversion of **10** to the Ni(II) porphyrin **3** was first attempted out using $Ni(acac)_2$ in toluene. Although quantitative metallation was achieved, purification was difficult due to presence of $Ni(acac)_2$, which led to an isolated yield for **3** of only 31%. Changing the metallation conditions from $Ni(acac)_2$ in toluene to $Ni(OAc)_2{\cdot}4H_2O$ in $MeOH/CHCl_3$, however, afforded the desired porphyrin **3** in 95% yield. Archipelago model compound **4** was synthesized *via* Sonogashira reaction of 1-ethynylpyrene with 2,6-dibromopyridine and subsequent hydrogenation, as reported previously.[55]

Aggregation in solution

Before exploring aggregation of porphyrin **3** with archipelago model compound **4**, a series of control experiments were done. First, phenylacetic acid was used as a simple carboxylic acid in a NMR titration experiment with pyridine in benzene-d_6 at 24 ± 2 °C (while toluene is more commonly used for aggregation studies, the symmetrical structure of benzene allows more facile analysis of ^{1}H NMR spectra due to the reduced number of signals from the solvent). Specifically, addition of pyridine (1 to 8 equivalents) to a 2.5 mM solution of phenylacetic acid gave changes in the ^{1}H NMR chemical shift for the signal of the methylene protons of phenylacetic acid (see ESI†). Nonlinear curve fitting for the chemical shift data with a 1 : 1 binding model gave an association constant $K_{assoc} = 123 \pm 12\ M^{-1}$.

In a second experiment, phenylacetic acid was titrated with model compound **4**,[56] rather than pyridine. At first, a 2.5 mM solution of phenylacetic acid was used for the titration with **4**. Limited by the solubility of **4**, only up to 4 equivalents could be added. As only weak binding was observed, a second titration with a 1.25 mM solution of phenylacetic acid was performed allowing addition up to 8 equivalents of **4**. Both titrations gave concentration dependent changes for the chemical shift for the signal of the methylene protons of phenylacetic acid, but the binding was quite lower compared to pyridine, with an averaged $K_{assoc} = 24 \pm 8\ M^{-1}$ (see ESI†), obtained from the two titrations detailed above. In general, it is know that substitution in the 2,6-positions of the pyridyl-ring has an impact on basicity, *e.g.*, for pyridine, 2,6-lutidine, and 2,6-diisopropylpyridine, $pK_a = 4.38$, 5.77, and 5.34, respectively.[57] Likewise, substitution also causes steric repulsion inhibiting hydrogen bonding.[57] Thus, the observed decrease in K_{assoc} going from pyridine to model compound **4** is likely explained by a combination of steric and electronic effects, as described in detail by Kitao and Jarboe for simple pyridine derivatives.[57]

Turning attention to the porphyrin carboxylic acid **3**, dilution titrations were first investigated by ^{1}H NMR spectroscopy to determine self-association. It was clear from these titrations that porphyrin **3** forms a dimeric species in benzene-d_6, and chemical shift analysis and fitting from multiple signals gave a dimerization constant of $K_{dim} = 390 \pm 27\ M^{-1}$ (see ESI†).

Finally, a ^{1}H NMR titration experiment was done with porphyrin **3** by addition of pyridine (1 to 8 equivalents). Fitting of the chemical shifts from multiple signals and considering $K_{dim} = 390 \pm 27\ M^{-1}$ for **3**, $K_{assoc} = 178 \pm 18\ M^{-1}$ was determined (see ESI†), which was comparable to the binding experiment between phenylacetic acid and pyridine (*vide supra*).

The interactions between model compounds **3** and **4** were then explored, using an analogous set of conditions for both the titration and ^{1}H NMR chemical shift analysis. Namely, the concentration of porphyrin **3** was kept constant at 2.5 mM, and the concentration of model compound **4** was varied from a minimum of 1.25 mM to a maximum of 10 mM (this was the solubility limit of **4**). The signals of the two methylene groups of **4** (H_b and H_c, see Fig. 2) shifted upfield from 3.86/3.34 (H_c/H_b) to 3.78/3.29 (H_c/H_b) ppm upon addition of 0.5 equivalents **4** to the porphyrin solution (Fig. 3), whereas further addition of **4** resulted in less significant downfield shifts. The signal of the methylene group protons of **3** (H_a, see Fig. 2) shifted downfield upon addition of **4**, from 3.20 ppm to a maximum of 3.43 ppm, after addition of four equivalents of **4**.

The observed relationship between chemical shift and concentration is consistent with expected acid–base interactions between the carboxylic acid functionality of **3** and the basic nitrogen of **4**. The chemical shifts for multiple signals upon titration of **3** with **4** were fit to a 1 : 1 binding model, suggesting a K_{assoc} = 316 ± 32 M^{-1} (Fig. 4). The 1 : 1 binding model is also supported by the presence of a weak signal for a 1 : 1 complex between **3** and **4** in the high resolution APPI mass spectrum (see ESI†).

To further investigate the nature of the complex formed between **3** and **4** in solution, Job's method of continuous variation was used.[58,59] Interestingly, the maximum is observed in the Job's plot at a mole fraction of 0.3 for **3**, suggesting a 1 : 2 complex between the porphyrin acid **3** and model compound **4**, respectively. Nonlinear curve fitting, considering both binding events, namely self-association of **3** (K_{dim} = 390 ± 27 M^{-1}) and a 1 : 2 binding model, results in an overall association constant of 1.23 ± 0.1 × 10^6 M^{-2}.[60]

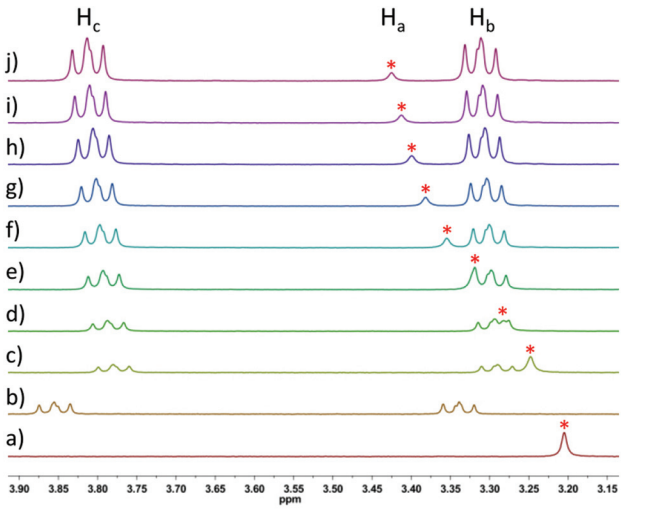

Fig. 3 ^{1}H NMR titration of **3** (2.5 mM constant) with increasing amounts of **4** in benzene-d_6; (a) **3** (2.5 mM); (b) **4** (1.25 mM); (c) **3** : **4** = 2 : 1; (d) **3** : **4** = 1 : 1; (e) **3** : **4** = 1 : 1.5; (f) **3** : **4** = 1 : 2; (g) **3** : **4** = 1 : 2.5; (h) **3** : **4** = 1 : 3; (i) **3** : **4** = 1 : 3.5; (j) **3** : **4** = 1 : 4; * = signal of the methylene group protons H_a of **3**; see Fig. 2 for proton assignment.

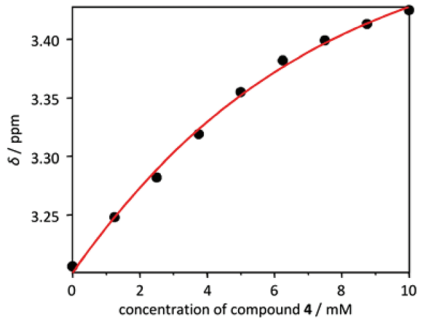

Fig. 4 Concentration dependent chemical shifts for the signal of the methylene group protons of porphyrin **3** upon titration with **4** and fitting to a 1 : 1 binding model.

The formation of a 1 : 2 complex between model compounds **3** and **4** would be in line with the results of Tan *et al.*, who report formation of a dimer for the ethano-linked pyrene substituted 2,2′-bipyridine derivative **2** (in $CDCl_3$),[15] which shares a structure similar to that of **4**. It has also been shown that dimerization of **2** is enhanced by the addition of water, which had the effect of forming an intermolecular bridge between bipyridyl groups.[30] It is, thus, reasonable that the carboxylic acid functionality of porphyrin **3** might mediate similar interactions between **4**, by bridging between two pyridyl-units, as in the role of water for the dimerization of **2**. The suggested stoichiometry from the Job's plot must be interpreted with caution, however, due to the self-association of porphyrin **3**. Thus, it is not possible at this point to unambiguously declare the nature of the interaction between **3** and **4**.

Conclusions

We have synthesized a new metalloporphyrin bearing an alkyl carboxylic acid (**3**), and specific aspects of asphaltene aggregation have been studied using this porphyrin. NMR spectroscopic analyses document the self-dimerization of the porphyrin carboxylic acid **3** in benzene-d_6, as well as aggregation of **3** with an asphaltene model compound that bears a basic pyridine group (*i.e.*, archipelago **4**). A Job's plot analysis between **3** and **4** suggests a 1 : 2 complex, but the exact nature of the association cannot be categorically established, due mainly to the self-association (self-dimerization) of porphyrin acid **3**.

While the stoichiometry of the **3**/**4** complex remains unresolved, this study does clearly show that the interactions between **3** and **4** are stronger than those of the individual model compound with either a simple base or acid, respectively. That is to say that the K_{assoc} determined for **3** with pyridine (178 ± 18 M^{-1}) and **4** with phenylacetic acid (24 ± 8 M^{-1}) are weaker than for **3** and **4** together, regardless of whether a 1 : 1 or 1 : 2 complex is formed. Based on our results, we hypothesize that the enhanced aggregation observed for **3** and

4 originates from the presence of additional intermolecular forces beyond the expected acid–base interactions (*e.g.*, π-stacking, hydrogen bonding), as suggested in the archipelago model.[8] Further analysis by both experiment and theoretical calculations are underway.

Experimental section

General

All chemicals and solvents were used as received from commercial suppliers. 1-Ethynylpyrene was prepared according to literature.[61] For the aldehyde synthesis, dry THF was distilled from sodium/benzophenone and DMF "with molecular sieve" (water <50 ppm) from Acros Organics was used. Solvent ratios are given as volume : volume. NMR spectra were recorded on a Bruker Avance 300 operating at 300 MHz (^{1}H NMR) and 75 MHz (^{13}C NMR), or a Bruker Avance 400 operating at 400 MHz (^{1}H NMR) and 100 MHz (^{13}C NMR), or a Jeol GX 400 operating at 100 MHz (^{13}C NMR) at rt, if not otherwise specified. Signals were referenced to residual solvent peaks (δ in parts per million (ppm) ^{1}H: $CDCl_3$, 7.26 ppm; C_6D_6, 7.16 ppm; ^{13}C: $CDCl_3$, 77.0 ppm; C_6D_6, 128.0 ppm). Coupling constants were assigned as observed. Mass spectra were recorded from Bruker micro TOF II (ESI) and Bruker maxis 4G (APPI) instruments. IR spectra were recorded on a Varian 660-IR spectrometer. UV-vis spectra were recorded on a Varian Cary 5000 UV-vis spectrophotometer (λ in nm; ε in M^{-1} cm^{-1}). TLC analysis was carried out with TLC plates from Macherey-Nagel (ALUGRAM® SIL G/UV_{254}) and visualized by UV-light of 254 nm or 366 nm. Silica Gel 60 M (0.04–0.063 mm) for column chromatography was purchased from Macherey-Nagel.

Compound 4. 1-Ethynylpyrene (0.491 g, 2.17 mmol) was added to a deoxygenated solution of 2,6-dibromopyridine (0.222 g, 0.937 mmol) in THF (70 mL) and diisopropylamine (10 mL). $PdCl_2(PPh_3)_2$ (0.127 g, 0.181 mmol) and CuI (0.052 g, 0.27 mmol) were sequentially added and the solution stirred at reflux for 16 h under a N_2-atmosphere. The solvents were removed *in vacuo*, and the resulting solid was washed with MeOH (5 × 20 mL), H_2O (5 × 20 mL), MeOH (2 × 20 mL), hexanes (50 mL), and dried *in vacuo*. The crude product, toluene (300 mL), and Pd/C (10%, 0.050 g) were added to a flask. The flask was fitted with a balloon filled with H_2 (*ca.* 15 psi), purged with H_2 (3 times), and stirred at rt for 3 d. The heterogeneous mixture was filtered over Celite and the solvent removed. Purification by column chromatography (silica gel, $CHCl_3$/hexanes 4 : 1) afforded compound **4** as a yellow solid (0.366 g, 73%). Mp 186–187 °C. R_f = 0.18 ($CHCl_3$/hexanes 4 : 1). IR (ATR) 3037 (w), 2924 (w), 1708 (w), 1579 (m), 1453 (m) cm^{-1}; ^{1}H NMR (300 MHz, $CDCl_3$) δ 8.35 (d, J = 9.3 Hz, 2H), 8.14 (d, J = 7.6 Hz, 4H), 8.11–7.94 (m, 10H), 7.83 (d, J = 7.8 Hz, 2H), 7.32 (t, J = 7.7 Hz, 1H), 6.80 (d, J = 7.7 Hz, 2H), 3.88–3.83 (m, 4H), 3.48–3.43 (m, 4H); ^{1}H NMR (400 MHz, C_6D_6) δ 8.38 (d, J = 9.2 Hz, 2H), 7.97–7.90 (m, 8H), 7.85–7.73 (m, 8H), 6.89 (t, J = 7.6 Hz, 1H), 6.51 (d, J = 7.6 Hz, 2H), 3.87–3.83 (m, 4H), 3.36–3.32 (m, 4H); ^{13}C NMR (75 MHz, $CDCl_3$) δ 160.4, 135.7, 131.4, 130.9, 129.9, 128.7, 127.5, 127.34, 127.31, 126.6, 125.8, 125.01, 124.97, 124.9, 124.8, 124.7, 123.4, 120.8, 39.8, 33.6 (one signal coincident or not observed); ^{13}C NMR (100 MHz, C_6D_6) δ 161.1, 136.6, 136.3, 132.0, 131.5, 130.5, 129.3, 128.6, 127.0, 126.0, 125.8, 125.7, 125.2, 125.1, 123.9, 120.5, 40.7, 33.9 (three signals coincident or not observed); ^{13}C–^{1}H HSQC (400 MHz, C_6D_6, selected correlations) δ 136.3 ↔ 6.89; 120.5 ↔ 6.51; 40.7 ↔ 3.36–3.32; 33.9 ↔ 3.87–3.83; ^{13}C–^{1}H HMBC (400 MHz, C_6D_6, selected correlations) δ 161.1 ↔ 6.89, 6.51, 3.87–3.83, 3.36–3.32; 136.6 ↔ 8.38, 7.97–7.90, 3.87–3.83, 3.36–3.32; 120.5 ↔ 6.51, 3.36–3.32; 40.7 ↔ 6.51, 3.87–3.83; 33.9 ↔ 3.36–3.32. APPI HRMS m/z calcd for $C_{41}H_{30}N$ ($[M + H]^+$) 536.2373, found 536.2374.

2-Methoxymethyl benzaldehyde (5).[50] 1-Bromo-2-(methoxymethyl)benzene (1.50 g, 7.46 mmol) was dissolved in dry THF (75 mL) under a N_2-atmosphere. After cooling to −78 °C, *n*-BuLi (2.5 M in hexane, 3.6 mL, 9.0 mmol) was slowly added. After stirring for 1 h, DMF was added (0.82 g, 0.86 mL, 11 mmol), and the mixture was allowed to warm to rt while stirring over night for 16 h. The solution was poured into a mixture of brine and HCl (150 mL, 1 : 1) and extracted with Et_2O (2 × 75 mL). The combined organic layers were washed with H_2O (3 × 150 mL) and dried over $MgSO_4$. After filtration and removal of the solvent, the residue was dissolved in CH_2Cl_2 and filtered through a plug of silica gel. Evaporation of the solvent and drying *in vacuo* afforded the product **5** (0.695 g, 62%) as a yellow oil. R_f = 0.49 (hexanes/CH_2Cl_2 1 : 1). IR (ATR) 3067 (vw), 2983 (w), 2927 (w), 2874 (w), 2822 (w), 2736 (w), 1691 (s) 1599 (m), 1574 (m), 1451 (m) cm^{-1}; ^{1}H NMR (300 MHz, $CDCl_3$) δ 10.12 (s, 1H), 7.78–7.76 (m, 1H), 7.56–7.48 (m, 2H), 7.39 (td, J = 7.3 Hz, 1.4 Hz, 1H), 4.78 (s, 2H), 3.39 (s, 3H); ^{13}C (75 MHz, $CDCl_3$) δ 192.4, 140.5, 133.5, 133.0, 132.0, 127.7, 127.4, 71.5, 58.2. ESI HRMS m/z calcd for $C_9H_{11}O_2$ ($[M + H]^+$) 151.0754, found 151.0753.

Porphyrin 7a. In degassed CH_2Cl_2 (1.5 L), 4-*n*-butylbenzaldehyde (90% pure, 2.1 mL, 11 mmol), pyrrole (1.0 g, 1.0 mL, 15 mmol), and aldehyde **5** (0.563 g, 3.75 mmol) were dissolved under a N_2-atmosphere. After addition of EtOH (1.5 mL) and $BF_3{\cdot}OEt_2$ (0.24 g, 0.21 mL, 1.7 mmol), the solution was stirred for 1 h at rt. DDQ (3.41 g, 15.0 mmol) was added and the mixture stirred for 2 h at rt. The solution was concentrated by rotary evaporation and the residue filtered through a plug of silica gel (CH_2Cl_2). The black/purple solid obtained after removal of the solvent was purified by column chromatography (silica gel, hexanes/CH_2Cl_2 1 : 1) to afford the porphyrin **8** (0.430 g, 18%) as the first fraction and the porphyrin **7a** (0.445 g, 14%) as the second fraction as purple solids. Mp 226–228 °C. R_f = 0.59 (hexanes/CH_2Cl_2 1 : 1). UV-vis (CH_2Cl_2) λ_{max} (ε) 419 (569 000), 516 (21 000), 550 (9830), 590 (6480), 646 (5150) nm; IR (ATR) 3314 (w), 2951 (m), 2923 (m), 2858 (m), 1465 (m), 1346 (m) cm^{-1}; ^{1}H NMR (300 MHz, $CDCl_3$) δ 8.92–8.89 (m, 6H), 8.73 (d, J = 4.8 Hz, 2H), 8.20–8.09 (m, 7H), 7.97 (d, J = 7.2 Hz, 1H), 7.85 (td, J = 7.6 Hz, J = 1.2 Hz, 1H), 7.66 (td, J = 7.5 Hz, J = 1.2 Hz, 1H), 7.60–7.57 (m, 6H), 4.15 (s, 2H), 2.99 (t, J = 7.7 Hz, 6H), 2.89 (s, 3H), 1.94 (pent, J = 7.6 Hz, 6H), 1.62 (sext, J = 7.4 Hz, 6H), 1.13 (t, J = 7.3 Hz, 9H), −2.66

(br s, 2H); ^{13}C NMR (75 MHz, $CDCl_3$) δ 142.3, 140.19, 140.17, 139.5, 139.3, 134.6, 134.0, 131.1 (br), 130.7 (br), 128.6, 126.73, 126.69, 126.3, 125.5, 120.6, 120.3, 116.9, 72.7, 58.1, 35.7, 33.8, 22.6, 14.2 (12 signals coincident or not observed). APPI HRMS *m*/*z* calcd for $C_{58}H_{59}N_4O$ ($[M + H]^+$) 827.4683, found 827.4713.

Porphyrin 8.[53] Mp >300 °C. R_f = 0.85 (hexanes/CH_2Cl_2 1 : 1). IR (ATR) 3314 (w), 3020 (vw), 2951 (w), 2923 (m), 2854 (m), 1466 (w), 1347 (w) cm^{-1}; ^{1}H NMR (300 MHz, $CDCl_3$) δ 8.89 (s, 8H), 8.14 (d, J = 8.0 Hz, 8H), 7.57 (d, J = 8.0 Hz, 8H), 2.97 (t, J = 7.7 Hz, 8H), 1.98–1.88 (m, 8H), 1.61 (sext, J = 7.4 Hz, 8H), 1.12 (t, J = 7.3 Hz, 12H), −2.71 (s, 2H); ^{13}C NMR (100 MHz, $CDCl_3$) δ 142.3, 139.5, 134.6, 130.9 (br), 126.7, 120.1, 35.7, 33.8, 22.6, 14.1 (1 signal coincident or not observed). ESI HRMS *m*/*z* calcd for $C_{60}H_{63}N_4$ ($[M + H]^+$) 839.5047, found 839.5053.

Porphyrin 9. To a solution of **7a** (58 mg, 0.070 mmol) in CH_2Cl_2 (15 mL), was added HBr in glacial HOAc (33%, 4.0 g, 8.5 mL, 49 mmol). The resulting dark green solution was stirred at rt. After 4 h, an additional amount of HBr in glacial HOAc (33%, 0.94 g, 2.0 mL, 12 mmol) was added and the mixture stirred at rt for 2 h. H_2O (50 mL) and CH_2Cl_2 (50 mL) were added. The organic layer was separated, washed with H_2O (100 mL), an aqueous saturated solution of $NaHCO_3$ (100 mL), and H_2O (100 mL). The organic phase was dried over $MgSO_4$ and filtered. The solvent was removed and the crude product **7b** (R_f = 0.67 (hexanes/CH_2Cl_2 1 : 1)) dried *in vacuo* and used without further purification. In PEG 400 (12 mL), the crude product **7b** was dissolved, KCN (0.452 g, 6.94 mmol) was added, and the mixture was stirred at rt for 24 h. CH_2Cl_2 (100 mL) and H_2O (100 mL) were added, the organic phase was separated and washed with H_2O (4 × 100 mL). After drying over $MgSO_4$, the mixture was filtered and the solvent removed. The residue was purified by column chromatography (silica gel, gradient hexanes/CH_2Cl_2 2 : 1 → 0 : 1) to afford the product **9** (51 mg, 89%) as a purple solid. Mp 180–182 °C. R_f = 0.41 (hexanes/CH_2Cl_2 1 : 1). UV-vis (CH_2Cl_2) λ_{max} (ε) 419 (546 000), 516 (21 100), 552 (10 000), 591 (6070), 646 (5440) nm; IR (ATR) 3314 (w), 2923 (m), 2855 (w), 1465 (m), 1346 (m) cm^{-1}; ^{1}H NMR (300 MHz, $CDCl_3$) δ 8.90–8.88 (m, 6H), 8.61 (d, J = 4.8 Hz, 2H), 8.17–8.08 (m, 7H), 7.98 (d, J = 7.2 Hz, 1H), 7.87 (td, J = 7.6 Hz, J = 1.3 Hz, 1H), 7.73 (t, J = 6.9 Hz, 1H), 7.57 (d, J = 8.1 Hz, 6H), 3.39 (s, 2H), 2.97 (t, J = 7.7 Hz, 6H), 1.92 (pent, J = 7.6 Hz, 6H), 1.60 (sext, J = 7.4 Hz, 6H), 1.10 (t, J = 7.3 Hz, 9H), −2.73 (s, 2H); ^{13}C NMR (75 MHz, $CDCl_3$) δ 142.4, 141.3, 139.3, 139.0, 134.6, 134.5, 134.3, 132.0, 131.2 (br), 129.3, 127.5, 126.8, 126.72, 126.65, 121.1, 120.6, 117.8, 115.0, 35.6, 33.8, 22.8, 22.6, 14.1 (12 signals coincident or not observed). ESI HRMS *m*/*z* calcd for $C_{58}H_{56}N_5$ ($[M + H]^+$) 822.4530, found 822.4513.

Porphyrin 10. Porphyrin **9** (39 mg, 0.047 mmol) was dissolved in AcOH (4 mL). H_2SO_4 (4 mL) and H_2O (1.3 mL) were added and the mixture heated to 95 °C for 90 h. The dark green solution was cooled to rt and poured into ice water (15 mL), whereupon a green precipitate formed. The solid was collected by filtration, washed with H_2O (50 mL), and dissolved in CH_2Cl_2 (50 mL). The solution was washed with H_2O (3 × 50 mL), a mixture of an aqueous saturated solution of $NaHCO_3$ and H_2O (2 : 1, 150 mL), and H_2O (50 mL). The solution was dried over $MgSO_4$ and filtered. The solvent was removed and the residue was purified by column chromatography (silica gel, CH_2Cl_2/EtOAc 9 : 1) to afford the product **10** (37 mg, 94%) as a purple solid. Mp 255–258 °C. R_f = 0.58 (CH_2Cl_2/acetone 19 : 1). UV-vis (THF) λ_{max} (ε) 418 (567 000), 514 (22 500), 549 (10 800), 592 (6220), 647 (4550) nm; IR (ATR) 3314 (w), 3021 (w), 2953 (m), 2924 (m), 2855 (m), 1707 (m), 1467 (m), 1347 (m) cm^{-1}; ^{1}H NMR (300 MHz, $CDCl_3$) δ 8.86 (d, J = 4.9 Hz, 2H), 8.83 (d, J = 4.8 Hz, 2H), 8.77 (d, J = 4.8 Hz, 2H), 8.61 (d, J = 4.8 Hz, 2H), 8.14–8.00 (m, 7H), 7.76–7.68 (m, 1H), 7.58 (t, J = 8.9 Hz, 4H), 7.49 (d, J = 7.4 Hz, 2H), 7.36 (d, J = 6.8 Hz, 2H), 3.37 (s, 2H), 2.97 (t, J = 7.7 Hz, 2H), 2.85 (t, J = 7.6 Hz, 4H), 1.97–1.78 (m, 6H), 1.67–1.47 (m, 6H), 1.13–1.03 (m, 9H), −2.74 (br s, 2H); ^{13}C NMR (100 MHz, $CDCl_3$) δ 175.4, 142.3, 142.2, 141.9, 139.5, 139.2, 135.4, 134.6, 134.51, 134.46, 134.41, 131.1 (br), 129.3, 128.6, 126.7, 126.6, 125.5, 120.6, 120.3, 116.7, 38.9, 35.7, 35.6, 33.8, 33.7, 22.63, 22.58, 14.14, 14.10 (6 signals coincident or not observed). ESI HRMS *m*/*z* calcd for $C_{58}H_{57}N_4O_2$ ($[M + H]^+$) 841.4476, found 841.4476; *m*/*z* calcd for $C_{58}H_{56}N_4NaO_2$ ($[M + Na]^+$) 863.4296, found 863.4314.

Porphyrin 3. Porphyrin **10** (14.7 mg, 0.0175 mmol) was dissolved in $CHCl_3$ (20 mL), and a solution of $Ni(OAc)_2{\cdot}4H_2O$ (0.100 g, 0.402 mmol) in MeOH (5 mL) was added. After heating to reflux for 24 h in the dark, the solution was cooled to rt, washed with H_2O (2 × 50 mL), a mixture of H_2O and an aqueous saturated solution of $NaHCO_3$ (9 : 1, 50 mL), and H_2O (50 mL). The organic layer was dried over $MgSO_4$ and filtered. After removal of the solvent, the residue was purified by column chromatography (silica gel, gradient CH_2Cl_2/acetone 1 : 0 → 15 : 1) to yield the product **3** (15.0 mg, 95%) as a red-purple solid. Mp 256–259 °C. R_f = 0.81 (CH_2Cl_2/acetone 19 : 1). UV-vis (CH_2Cl_2) λ_{max} (ε) 415 (312 000), 528 (22 100) nm; IR (ATR) 3023 (w), 2953 (s), 2926 (s), 2859 (m), 1709 (m), 1460 (m), 1352 (m) cm^{-1}; ^{1}H NMR (300 MHz, $CDCl_3$) δ 8.76 (d, J = 5.0 Hz, 2H), 8.73 (d, J = 5.0 Hz, 2H), 8.68 (d, J = 5.0 Hz, 2H), 8.51 (d, J = 4.9 Hz, 2H), 7.96–7.82 (m, 7H), 7.69–7.63 (m, 1H), 7.55 (t, J = 6.9 Hz, 2H), 7.48 (d, J = 8.2 Hz, 2H), 7.38 (d, J = 8.2 Hz, 4H), 3.24 (s, 2H), 2.90 (t, J = 7.7 Hz, 2H), 2.82 (t, J = 7.7 Hz, 4H), 1.91–1.74 (m, 6H), 1.62–1.44 (m, 6H), 1.09–1.01 (m, 9H); ^{13}C NMR (100 MHz, $CDCl_3$) δ 175.2, 142.9, 142.8, 142.4, 142.34, 142.27, 140.6, 138.1, 138.0, 134.9, 133.9, 133.64, 133.59, 132.5, 132.21, 132.17, 131.5, 129.3, 128.6, 126.9, 126.8, 125.7, 119.3, 119.1, 115.8, 38.6, 35.6, 35.5, 33.8, 33.7, 22.6, 22.5, 14.10, 14.07 (1 signal coincident or not observed). ESI HRMS *m*/*z* calcd for $C_{58}H_{54}N_4NaNiO_2$ ($[M + Na]^+$) 919.3493, found 919.3486; *m*/*z* calcd for $C_{58}H_{53}N_4Na_2NiO_2$ ($[M - H + 2Na]^+$) 941.3312, found 941.3303.

Acknowledgements

We are grateful for financial support from the Institute for Oil Sands Innovation at the University of Alberta, the Natural Sciences and Engineering Research Council of Canada, and the Graduate School Molecular Science (GSMS) at FAU. We thank Dr. Alexander Scherer for his assistance, as well as Prof.

Jürgen Schatz and Dr. Max von Delius for helpful discussions regarding assessment of the binding constants.

Notes and references

1 K. Aleklett, M. Höök, K. Jakobsson, M. Lardelli, S. Snowden and B. Söderbergh, *Energy Policy*, 2010, **38**, 1398–1414.
2 M. R. Gray and W. C. McCaffrey, *Energy Fuels*, 2002, **16**, 756–766.
3 I. Gawel, D. Bociarska and P. Biskupski, *Appl. Catal., A*, 2005, **295**, 89–94.
4 N. Haji-Akbari, P. Teeraphapkul and H. S. Fogler, *Energy Fuels*, 2014, **28**, 909–919.
5 S. Chiaberge, G. Guglielmetti, L. Montanari, M. Salvalaggio, L. Santolini, S. Spera and P. Cesti, *Energy Fuels*, 2009, **23**, 4486–4495.
6 R. R. Chianelli, K. Castillo, V. Gupta, A. M. Qudah, B. Torres and R. E. Abujnah, *Asphaltene based photovoltaic devices. US Patent* 2014/0234026, 2014.
7 S. M. Hashmi, K. X. Zhong and A. Firoozabadi, *Soft Matter*, 2012, **8**, 8778–8785.
8 M. R. Gray, R. R. Tykwinski, J. M. Stryker and X. Tan, *Energy Fuels*, 2011, **25**, 3125–3134.
9 M. P. Hoepfner and H. S. Fogler, *Langmuir*, 2013, **29**, 15423–15432.
10 T. E. Havre and J. Sjöblom, *Colloids Surf., A*, 2003, **228**, 131–142.
11 S. B. Jaffe, H. Freund and W. N. Olmstead, *Ind. Eng. Chem. Res.*, 2005, **44**, 9840–9852.
12 J. G. Speight, *Oil Gas Sci. Technol.*, 2004, **59**, 467–477.
13 O. C. Mullins, H. Sabbah, J. Eyssautier, A. E. Pomerantz, L. Barré, A. B. Andrews, Y. Ruiz-Morales, F. Mostowfi, R. McFarlane, L. Goual, R. Lepkowicz, T. Cooper, J. Orbulescu, R. M. Leblanc, J. Edwards and R. N. Zare, *Energy Fuels*, 2012, **26**, 3986–4003.
14 F. Rakotondradany, H. Fenniri, P. Rahimi, K. L. Gawrys, P. K. Kilpatrick and M. R. Gray, *Energy Fuels*, 2006, **20**, 2439–2447.
15 X. Tan, H. Fenniri and M. R. Gray, *Energy Fuels*, 2008, **22**, 715–720.
16 Z. Wang, W. Liang, G. Que and J. Qian, *Pet. Sci. Technol.*, 1997, **15**, 559–577.
17 O. P. Strausz, P. Peng and J. Murgich, *Energy Fuels*, 2002, **16**, 809–822.
18 O. P. Strausz, T. W. Mojelsky, E. M. Lown, I. Kowalewski and F. Behar, *Energy Fuels*, 1999, **13**, 228–247.
19 P. M. Spiecker, K. L. Gawrys, C. B. Trail and P. K. Kilpatrick, *Colloids Surf., A*, 2003, **220**, 9–27.
20 K. L. Gawrys, G. A. Blankenship and P. K. Kilpatrick, *Langmuir*, 2006, **22**, 4487–4497.
21 J. M. Sheremata, M. R. Gray, H. D. Dettman and W. C. McCaffrey, *Energy Fuels*, 2004, **18**, 1377–1384.
22 J. Murgich, J. A. Abanero and O. P. Strausz, *Energy Fuels*, 1999, **13**, 278–286.
23 R. I. Rueda-Velásquez, H. Freund, K. Qian, W. N. Olmstead and M. R. Gray, *Energy Fuels*, 2013, **27**, 1817–1829.
24 A. Karimi, K. Qian, W. N. Olmstead, H. Freund, C. Yung and M. R. Gray, *Energy Fuels*, 2011, **25**, 3581–3589.
25 A. Scherer, F. Hampel, M. R. Gray, J. M. Stryker and R. R. Tykwinski, *J. Phys. Org. Chem.*, 2012, **25**, 597–606.
26 S. Tanaka, M. Shirakawa, K. Kaneko, M. Takeuchi and S. Shinkai, *Langmuir*, 2005, **21**, 2163–2172.
27 F. Sguerra, V. Bulach and M. W. Hosseini, *Dalton Trans.*, 2012, **41**, 14683–14689.
28 Y. K. Kryschenko, S. R. Seidel, A. M. Arif and P. J. Stang, *J. Am. Chem. Soc.*, 2003, **125**, 5193–5198.
29 K. Akbarzadeh, D. C. Bressler, J. Wang, K. L. Gawrys, M. R. Gray, P. K. Kilpatrick and H. W. Yarranton, *Energy Fuels*, 2005, **19**, 1268–1271.
30 X. Tan, H. Fenniri and M. R. Gray, *Energy Fuels*, 2009, **23**, 3687–3693.
31 J. Wang, N. van der T. Opedal, Q. Lu, Z. Xu, H. Zeng and J. Sjöblom, *Energy Fuels*, 2012, **26**, 2591–2599.
32 H. Sabbah, A. E. Pomerantz, M. Wagner, K. Müllen and R. N. Zare, *Energy Fuels*, 2012, **26**, 3521–3526.
33 B. Breure, D. Subramanian, J. Leys, C. J. Peters and M. A. Anisimov, *Energy Fuels*, 2013, **27**, 172–176.
34 Y. Ruiz-Morales and O. C. Mullins, *Energy Fuels*, 2007, **21**, 256–265.
35 Y. Ruiz-Morales, X. Wu and O. C. Mullins, *Energy Fuels*, 2007, **21**, 944–952.
36 L. M. da Costa, S. Hayaki, S. R. Stoyanov, S. Gusarov, X. Tan, M. R. Gray, J. M. Stryker, R. Tykwinski, J. W. de M. Carneiro, H. Sato, P. R. Seidl and A. Kovalenko, *Phys. Chem. Chem. Phys.*, 2012, **14**, 3922–3934.
37 L. M. da Costa, S. R. Stoyanov, S. Gusarov, X. Tan, M. R. Gray, J. M. Stryker, R. Tykwinski, J. W. de M. Carneiro, P. R. Seidl and A. Kovalenko, *Energy Fuels*, 2012, **26**, 2727–2735.
38 S. Mitra-Kirtley, O. C. Mullins, J. van Elp, S. J. George, J. Chen and S. P. Cramer, *J. Am. Chem. Soc.*, 1993, **115**, 252–258.
39 A. Treibs, *Liebigs Ann. Chem.*, 1934, **509**, 103–114.
40 A. Treibs, *Liebigs Ann. Chem.*, 1934, **510**, 42–62.
41 A. Treibs, *Liebigs Ann. Chem.*, 1935, **517**, 172–196.
42 A. Treibs, *Angew. Chem.*, 1936, **49**, 682–686.
43 G. P. Dechaine and M. R. Gray, *Energy Fuels*, 2010, **24**, 2795–2808.
44 C.-X. Yin, X. Tan, K. Müllen, J. M. Stryker and M. R. Gray, *Energy Fuels*, 2008, **22**, 2465–2469.
45 S. D. Cardozo, M. Schulze, R. R. Tykwinski and M. R. Gray, *Energy Fuels*, 2015, **29**, 1494–1502.
46 P. S. Clezy, *Aust. J. Chem.*, 1991, **44**, 1163–1193.
47 T. D. Lash, *Energy Fuels*, 1993, **7**, 166–171.
48 B. E. Smith and T. D. Lash, *Tetrahedron*, 2010, **66**, 4413–4422.
49 The assignment of H_b and H_c was possible by 2D NMR spectroscopic measurements, primarily using long range

correlations of H_b and H_c to the carbons of the pyridyl ring (see ESI†).
50 B. Christenson, G. Hallnemo and C. Ullenius, *Tetrahedron*, 1991, **47**, 4739–4752.
51 J. S. Lindsey, I. C. Schreiman, H. C. Hsu, P. C. Kearney and A. M. Marguerettaz, *J. Org. Chem.*, 1987, **52**, 827–836.
52 N. Jux, *Org. Lett.*, 2000, **2**, 2129–2132.
53 W. M. Campbell, K. W. Jolley, P. Wagner, K. Wagner, P. J. Walsh, K. C. Gordon, L. Schmidt-Mende, M. K. Nazeeruddin, Q. Wang, M. Grätzel and D. L. Officer, *J. Phys. Chem. C*, 2007, **111**, 11760–11762.
54 S. Jasinski, E. A. Ermilov, N. Jux and B. Röder, *Eur. J. Org. Chem.*, 2007, 1075–1084.
55 A. H. Alshareef, A. Scherer, X. Tan, K. Azyat, J. M. Stryker, R. R. Tykwinski and M. R. Gray, *Energy Fuels*, 2012, **26**, 1828–1843.
56 No evidence for self-association was found (see ESI†).
57 T. Kitao and C. H. Jarboe, *J. Org. Chem.*, 1967, **32**, 407–410.
58 K. Hirose, *J. Inclusion Phenom. Macrocyclic Chem.*, 2001, **39**, 193–209.
59 E. J. Olson and P. Bühlmann, *J. Org. Chem.*, 2011, **76**, 8406–8412.
60 S. Natesan, T. Wang, V. Lukacova, V. Bartus, A. Khandelwal and S. Balaz, *J. Chem. Inf. Model.*, 2011, **51**, 1132–1150.
61 M. Hissler, A. Harriman, A. Khatyr and R. Ziessel, *Chem. – Eur. J.*, 1999, **5**, 3366–3381.